

## CHAPTER 3

### **Finding transition pathways: throwing ropes over rough mountain passes, in the dark**

DAVID CHANDLER

*Department of Chemistry, University of California, Berkeley, CA 94720*

from: *Classical and Quantum Dynamics in Condensed Phase Simulations*, edited by  
B. J. Berne, G. Ciccotti and D. F. Coker (World Scientific, Singapore, 1998), pgs. 51-66.



**Contents**

<b>1</b>	<b>– Locating transition states</b>	<b>55</b>
<b>2</b>	<b>– Directed paths or chains of states</b>	<b>57</b>
<b>3</b>	<b>– Transition probabilities</b>	<b>59</b>
<b>4</b>	<b>– Illustrative examples</b>	<b>61</b>
<b>5</b>	<b>– Summary</b>	<b>65</b>



### 1. – Locating transition states

Figure 1 illustrates a trajectory passing over a barrier separating two stable states,  $A$  and  $B$ . If we know the location of the bottleneck, the dynamics of the rare event is solved by initiating trajectories from that bottleneck. But what if the bottleneck is not known? What if it is not even specifiable in terms of a small number of coordinates? Such is the case for most high dimensional systems. How then can a rare event be studied? This lecture addresses this question.

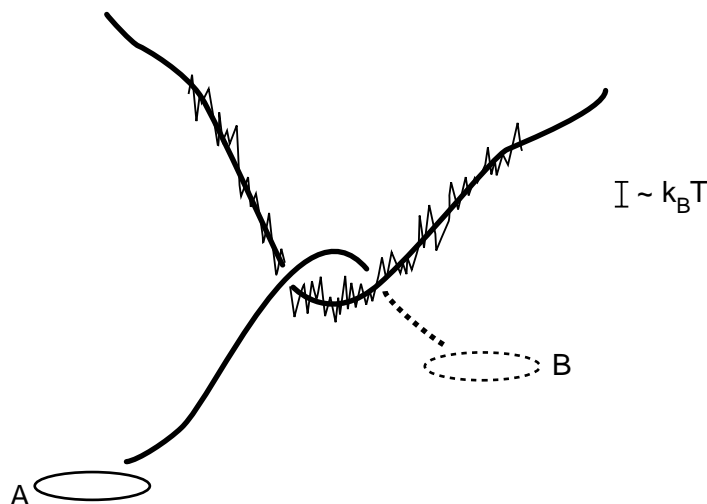


Fig. 1. – Schematic pathway between stable states  $A$  and  $B$ . The light rugged line indicates the roughness that generally characterizes the potential energy surface of a high dimensional system.

Consider, for example, the dissociation of NaCl in water. It seems natural to characterize the stable states in terms of the Na-Cl separation,  $r$ . The bound species corresponds to a range of small  $r$  values — where the potential of mean force between the  $\text{Na}^+$  and  $\text{Cl}^-$  ions,  $w_{\text{Na}^+\text{Cl}^-}(r)$ , has its first and most pronounced minimum. Beyond that region of  $r$  values, the species can be regarded as dissociated. It might seem similarly natural to also use  $r$  as the reaction coordinate describing the kinetics of the dissociation. But it is not likely that  $r$  captures the dynamics of the rate determining step. Indeed, much like the mechanism of electron transfer, the dissociation of NaCl is likely propelled by reorganization of the surrounding water — reorganization that will solvate the dissociated ions in preference to the associated NaCl molecule. Unlike the electron transfer case, however, a single collective coordinate that captures the nature of this solvent reorganization is not known.

Reasonable sampling statistics requires reasonable access to the coordinates that

control the dynamics. In Fig.2, for example, a coordinate  $q$  serves as the “order parameter” characterizing the stable states (as  $r$  characterizes the bound and dissociated states of NaCl). But, a second coordinate,  $q'$ , is also important in the kinetics. In particular,  $q'$  determines the location of the transition state between the stable states. The reversible work or free energy of  $q$ ,  $F(q)$ , is maximum at a point that is far from the transition state. Thus, if this extremum were chosen to initiate trajectories, few such trajectories would pass between the stable states, the resulting transmission coefficient would be very small, and its statistics would thus be relatively poor.

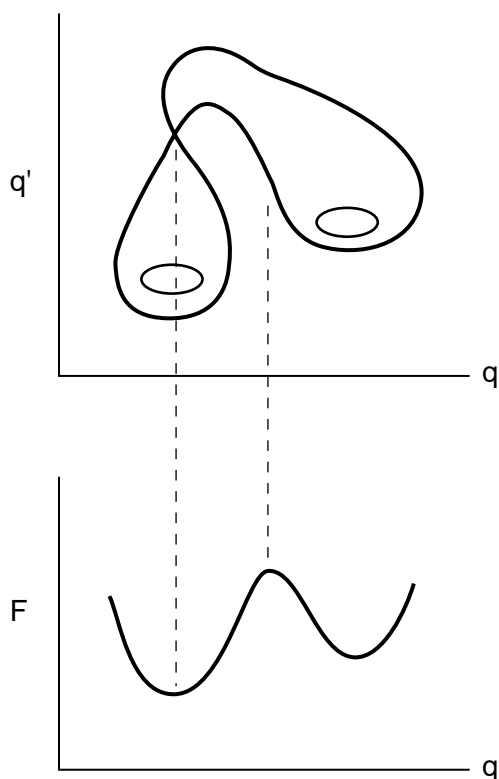


Fig. 2. – Topography of a potential energy surface,  $V(q, q')$  (upper graph), and the corresponding free energy,  $F(q)$  (lower graph). The latter is  $-k_B T$  times the logarithm of  $\sum_{q'} \exp[-\beta V(q, q')]$ . Note that a point of maximum free energy does not necessarily coincide with a saddle point or transition state in the potential energy surface.

The dissociation of NaCl in water illustrates the problem. The potential of mean force,  $w_{\text{Na}^+\text{Cl}^-}(r)$ , has a maximum at  $r^*$ , a point between the first and second coordination shells. As such,  $\theta(r^* - r)$ , the unit step function that is 1 when  $r < r^*$ , is a natural and simple definition of the population operator for the bound molecule. The calculation of the reactive flux crossing  $r = r^*$ ,

$$(1) \quad k(t) = \langle \dot{r} \delta(r - r^*) \theta[r(t) - r^*] \rangle / \langle \theta(r^* - r) \rangle ,$$

however, yields a plateau value that is very small compared to  $k(0^+)$ , so small that the computation is a nearly impractical route to determining the rate of dissociation. Even

when confined to  $r = r^*$ , trajectories that do lead to dissociation remain in the wings of the distribution. While the value of  $r$  can serve to characterize the stable state, other coordinates are evidently crucial to the kinetics of dissociation.

The topography chosen in Fig.2 illustrates the possible danger in adopting a satisfactory order parameter to serve also as a reaction coordinate. The example of NaCl dissociation in water shows that the topography is not far fetched. Another example is electron transfer in the inverted regime. See Fig.3. Here, solvent polarization is the order parameter, but monotonic progress of this variable does not lead the system to its transition state. Yet another example is capillary condensation. In this case, the bulk fluid density is the order parameter, but the kinetics of the condensation is controlled by interfacial fluctuations at the capillary surfaces.

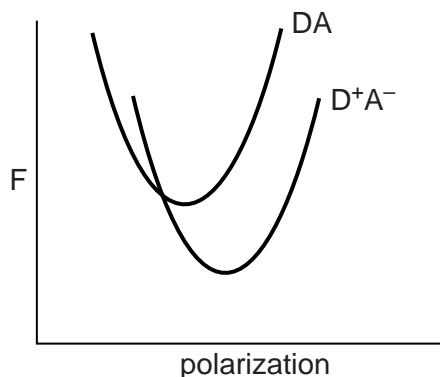


Fig. 3. – The free energy of two diabatic charge transfer states as functions of solvent nuclear polarization. They intersect in the inverted regime. For this case, polarization changes non-monotonically as the system passes from one stable state, through the transition state (where the two diabatic states intersect), to the other stable state.

Identifying reaction coordinates is closely related to finding effective saddle points on potential energy surfaces — the accessible mountain passes that separate deep valleys. For low dimensional systems, the explicit location of saddle points can be found numerically. For high dimensional systems, however, the potential energy surface can be rough on the scale of thermal energies,  $k_B T$ , as illustrated in Fig.1. In this case, the explicit locations of only a few specific saddle points are of little statistical importance. Rather than search for explicit saddle points, a useful strategy must effectively sample an ensemble of transition pathways.

## 2. – Directed paths or chains of states

Several years ago, Lawrence Pratt introduced a perspective with which this sampling can be performed. In particular, Pratt suggested focusing on the statistics of chains of states that were directed or biased to begin in one stable state and end in another. The idea can be expanded to a point where time correlation functions, like the reactive flux, can be calculated in much the same way that equilibrium distributions are calculated from umbrella sampling. The approach does require *a priori* specification of stable states, but it does not require preconceived notions of the mechanism for transitions between the stable states.

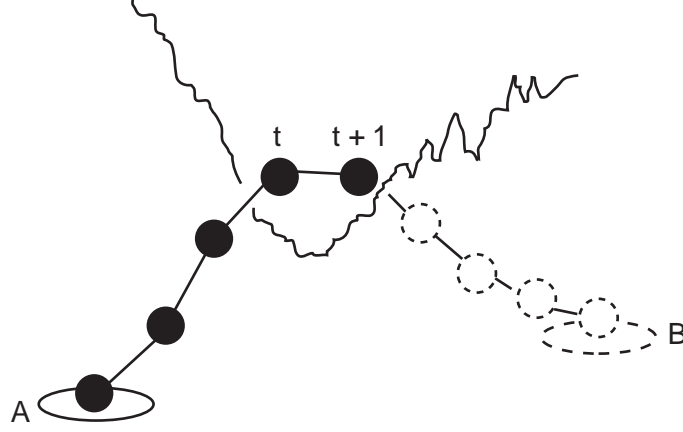


Fig. 4. – Schematic pathway between stable states  $A$  and  $B$ , with points on the path marked at discrete points in time.

To describe the general idea, consider the transition path drawn in Fig.1, but discretized in time as illustrated in Fig.4. Further, consider the probability distributions that describe the evolution of the system from one such time slice to another. At time slice  $t$ , the system is in configuration  $r_t$ . The time index is discrete with adjacent points separated by physical time  $\Delta\tau$ . Thus, time slice  $t$  corresponds to physical time  $t \Delta\tau$ . Let  $P(r_t, r_{t+1})$  denote the transition probability that in a time  $\Delta\tau$ , the system will move from configuration  $r_t$  to configuration  $r_{t+1}$ . Then, with  $\rho(r_0)$  denoting the equilibrium distribution for  $r_0$ ,

$$(2) \quad P[r(t)] = \rho(r_0) \prod_{t=0}^{L-1} P(r_t, r_{t+1})$$

is the probability functional for the sequence of configurations  $(r_0, r_1, \dots, r_L) \equiv r(t)$ . This sequence is a path of time duration  $\tau = L\Delta\tau$ . If the path coincides with physical dynamics, the transition probabilities will preserve the equilibrium distribution. That is,

$$(3) \quad \int dr_0 \int dr_1 \dots \int dr_{L-1} \rho(r_0) \prod_{t=0}^{L-1} P(r_t, r_{t+1}) = \rho(r_L).$$

For the equilibrium system, the (not normalized) probability functional for paths of time duration  $\tau$  originating in state  $A$  is

$$(4) \quad P_A[r(t)] = h_A(r_0) \rho(r_0) \prod_{t=0}^{L-1} P(r_t, r_{t+1}) \equiv \exp(-S_A[r(t)]),$$

where  $h_A(r)$  is 1 when  $r$  is a configuration corresponding to state  $A$ , and zero otherwise. Similarly, the distribution functional for paths that reach state  $B$  from state  $A$  in a time  $\tau$  is

$$(5) \quad P_{AB}[r(t)] = h_A(r_0) \rho(r_0) \left[ \prod_{t=0}^{L-1} P(r_t, r_{t+1}) \right] h_B(r_L) \equiv \exp(-S_{AB}[r(t)]),$$



where  $h_B(r)$  is 1 when  $r$  is a configuration corresponding to state  $B$ , and zero otherwise.

The general idea is to sample transition paths with the weight functionals  $P_A[r(t)]$  and  $P_{AB}[r(t)]$  and their associated action functionals,  $S_A[r(t)]$  and  $S_{AB}[r(t)]$ , defined in Eqs.(4) and (5). The efficiency of the sampling derives from the ability to reversibly control or direct paths from one stable state to another. In particular, with weight functionals like (4) and (5), the time correlation function resembles the ratio of two partition functions. For example,

$$(6) \quad \frac{\langle h_A h_B(\tau) \rangle}{\langle h_A \rangle} = \frac{\int Dr(t) h_A(r_0) \left[ \rho(r_0) \prod_{t=0}^{L-1} P(r_t, r_{t+1}) \right] h_B(r_\tau)}{\int Dr(t) h_A(r_0) \left[ \rho(r_0) \prod_{t=0}^{L-1} P(r_t, r_{t+1}) \right]} \\ = \frac{\int Dr(t) \exp(-S_{AB}[r(t)])}{\int Dr(t) \exp(-S_A[r(t)])} ,$$

where  $Dr(t)$  denotes  $dr_0 dr_1 \dots dr_L$ , and the integration,  $\int Dr(t)$  coincides with a sum or integration over all paths of duration  $\tau = L\Delta t$ .

From this perspective,

$$(7) \quad w_{AB}(\tau) = -\ln [\langle h_A h_B(\tau) \rangle / \langle h_A \rangle]$$

can be viewed as a reversible work. This fact follows from the conception of paths as isomorphic directed polymers. See Fig.5. The statistics for paths of time duration  $\tau$  is the same as Boltzmann statistics for chains with  $L = \tau/\Delta t$  segments. In this mapping, the “potential energy” for the isomorphic chains connecting states  $A$  and  $B$  is  $S_{AB}[r(t)]$ . Thus,  $w_{AB}(\tau)$  is an isomorphic free energy change produced by altering this potential energy from  $S_A[r(t)]$  to  $S_{AB}[r(t)]$ . In other words, the calculation of  $w_{AB}(\tau)$  is equivalent to calculating the reversible work to confine the last segments of the chains, given that the initial segments are confined to coincide with configurations where  $h_A(r_0) = 1$ . Furthermore, for a time  $\tau$  of the order of a plateau time,

$$(8) \quad \langle h_A h_B(\tau) \rangle / \langle h_A \rangle \sim k_{AB} \tau .$$

Thus, the calculation of the rate constant,  $k_{AB}$ , can be accomplished with the same techniques used to compute free energy changes, without reference to a specific transition state.

### 3. – Transition probabilities

To carry out the calculation sketched in the previous section, one must identify the transition probabilities appropriate to the dynamics of interest, and one must employ a computational algorithm that efficiently samples configurations of the isomorphic directed polymers. For the case of deterministic dynamics, such as the integration of Newton’s equations of motion, the procedure would correspond to roughly the following: *i.* Begin with some (perhaps arbitrarily chosen) initial path, with initial and final configurations lying in states  $A$  and  $B$ , respectively; *ii.* at random, choose a time slice on that path; *iii.* with the configuration at that time slice and randomly assigned velocities, run trajectories forward and backward in time, thus forming a new path; *iv.* accept or reject the new path (in the sense of a Monte Carlo move) in a fashion that will ultimately be

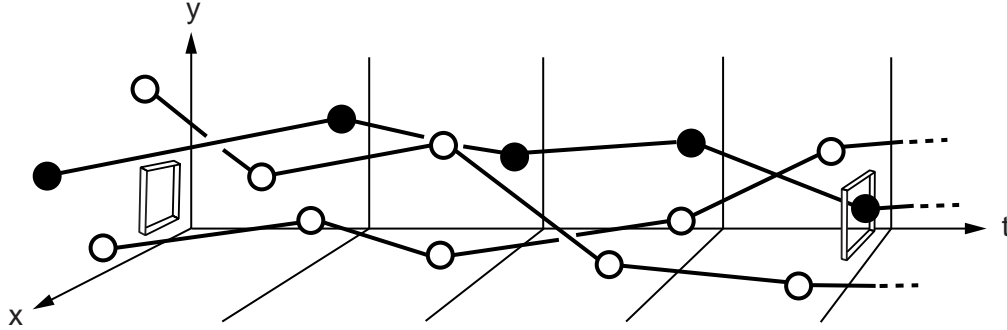


Fig. 5. – Schematic paths of three particles in a  $d = 2$  dimensional system. The configurations of the three particles are noted at five separate time slices (i.e., points in time). With time,  $t$ , as an additional dimension, these paths can be viewed as directed polymers in  $d + 1$  dimensions. For the pictured paths, in the first time slice, no particle resides in the boxed region of the  $x - y$  plane. In the fifth time slice, one particle resides in the boxed region. For the pictured paths, therefore, the initial and final states are characterized by the population operators  $h_A = 1$  and  $h_B = 1$ , respectively, where  $h_B$  is 1 when one particle resides in the boxed region, is zero otherwise, and  $h_A = 1 - h_B$ .

consistent with the distribution (5); *v.* with the path that remains from step *iv*, return to step *ii*, and continue the cycle over and over again. This type of algorithm should prove quite useful. For this lecture, however, we confine the discussion to paths generated by stochastic dynamics.

For example, in the case of Langevin dynamics in the high friction (non-inertial) limit, the equation of motion with unit mass is

$$(9) \quad \frac{dr}{d\tau} = F + \eta$$

where  $F = -\nabla U/\gamma$  is the systematic force divided by the friction constant, and  $\eta$  is the random force, obeying white noise Gaussian statistics. For a small enough time interval,  $\Delta t$ , integration gives

$$(10) \quad r_{t+1} = r_t + \Delta\tau F(r_t) + \delta r$$

where  $\delta r$ , the integral of  $\eta$  over the time interval, has the distribution

$$(11) \quad p(\delta r) \propto \exp[-(\delta r)^2/4D \Delta\tau] .$$

In this relationship,  $D = k_B T/\gamma$  is the diffusion constant. Its connection to temperature and the friction constant ensures that the trajectory advanced by Eq.(10) will preserve an equilibrium canonical distribution. The transition probability associated with this rule is

$$(12) \quad P(r_t, r_{t+1}) dr_{t+1} = p(r_{t+1} - r_t - \Delta\tau F_t) |\partial\delta r/\partial r_{t+1}| dr_{t+1} .$$

With Eq.(10), the Jacobian,  $|\partial\delta r/\partial r_{t+1}|$ , is unity. As such,

$$(13) \quad P(r_t, r_{t+1}) \propto \exp\{-[r_{t+1} - r_t - \Delta\tau F(r_t)]^2/4D \Delta\tau\} .$$

[On combining Eqs.(2) and (13), a subtlety is found in the continuum limit. In particular, a correction to Eq.(10) enters the analysis, leading to a nontrivial Jacobian factor. This factor produces the  $\nabla F$  contribution that is standard in the continuum path integral action for diffusion. Provided we maintain a discrete representation with small values of  $\Delta t$ , this subtlety should not play a role.]

Metropolis Monte Carlo provides another example of a stochastic trajectory. In this case

$$(14) \quad P(r_t, r_{t+1}) = w(r_t, r_{t+1}) + \Delta(r_t - r_{t+1}) Q(r_t),$$

where

$$(15) \quad w(r_t, r_{t+1}) = \eta(r_t, r_{t+1}) \min \{1, \exp(-\beta[E(r_{t+1}) - E(r_t)])\},$$

and

$$(16) \quad Q(r_t) = 1 - \sum_{r_{t+1}} w(r_t, r_{t+1}),$$

and  $\eta(r_t, r_{t+1})$  is the probability of trying  $r_{t+1}$  as a new configuration given  $r_t$  is the current configuration. The second term on the right-hand side of Eq.(14), the contribution with the Kronecker delta function,  $\Delta(r_t - r_{t+1})$ , gives the probability for rejecting a trial move. The first term gives the probability for accepting the trial move. The transition probability (14) is clearly normalized, and it preserves the canonical distribution, i.e.,

$$(17) \quad \sum_{r_t} \exp[-\beta E(r_t)] P(r_t, r_{t+1}) = \exp[-\beta E(r_{t+1})].$$

While (13) is useful for treating systems with continuous degrees of freedom, the transition probability (14) is also useful for treating discrete systems (e.g., Ising models).

As suggested by Fig.5, sampling with these probability functionals must overcome the possibility of significant entanglements. In other words, the chains of states move on a rough landscape, or more precisely, a rough “action-scape”. As such, diffusion of these chains will be slow and therefore impractical for some sampling algorithms, such as those generated through local (single particle) Monte Carlo procedures. On the other hand, satisfactory, if not optimal, sampling is obtained with the straightforward collective moves produced by treating the isomorphic chains as dynamical entities. We now turn to two illustrative examples as demonstrations.

#### 4. – Illustrative examples

##### Barrier crossing in a bi-stable potential

The simple two dimensional potential energy surface pictured in Fig.6 provides an example where transition path dynamics can be studied by straightforward trajectories and compared with that found by path sampling.

In particular, consider a trajectory run on this surface with the equation of motion (9). Since the dimensionality is low, it is not difficult to run this trajectory long enough for the occurrence of many transitions between the stable states. From such a trajectory, reasonable statistics for  $\langle h_A h_B(t) \rangle / \langle h_A \rangle$  can be obtained. A result acquired this way is graphed in Fig.7. The linear plateau region anticipated in Eq.(8) is apparent for times  $\tau \geq 100\Delta\tau$ .

Using the same potential energy and friction constant, paths can be sampled according to Eqs.(5) and (13), performing stochastic molecular dynamics trajectories of the isomorphic polymers. The isomorphic reversible work and thus  $\langle h_A h_B(t) \rangle / \langle h_A \rangle$  is obtained from this sampling by creating  $h_B$  in stages from small alterations of  $h_A$ . A result of this type of calculation is graphed in Fig.7. The result is indistinguishable from that found with straightforward trajectories, thus demonstrating that path sampling is correct in principle. The utility of path sampling in practice, however, is found in its capacity to explore pathways that cannot be conveniently illuminated by straightforward trajectories. We turn to such a case now.

### Transformation of a cold cluster

Consider a cluster of seven Lennard-Jones disks in two dimensions at the low temperature  $k_B T = 0.05\varepsilon$ , where  $\varepsilon$  is the depth of the Lennard-Jones pair potential. In its lowest potential energy configurations, one of the seven particles is surrounded by the other six particles, forming a regular hexagon, with nearest neighbor separation corresponding to the minimum of the Lennard-Jones potential. At the temperature  $0.05\varepsilon/k_B$ , the compact cluster remains stable for very long periods of time. Further, reorganization of its intracuster structure is rare. Indeed, on carrying out a trajectory of the low temperature cluster with Eq.(10), the central particle typically exchanges with one of its surrounding neighbors only once in  $10^{14}$  time steps.

Importance sampling of the ensemble of rare transformations is done by considering paths where the initial stable state  $A$  comprises configurations where, say, particle 1 is close to the center of mass of the cluster, and the final stable state  $B$  is where that same particle is roughly one Lennard-Jones disk diameter away from the center of mass. The most probable of such paths can be found by introducing an artificial temperature  $T^*$  into an altered path distribution

$$(18) \quad P_{AB}[r(t)] \rightarrow P_{AB}^*[r(t)] \equiv \exp(-S_{AB}[r(t)]/T^*).$$

Starting from a variety of configurations taken from trajectories of the isomorphic directed polymers, with potential energy  $S_{AB}[r(t)]$ , the isomorphic temperature can be lowered or quenched from  $T^* = 1$ , thereby emphasizing those paths (i.e., isomorphic polymer configurations) with the lowest action (i.e., lowest isomorphic potential energy).

For the seven particle cluster, the potential energy and action are relatively smooth, so that either quenching or annealing  $T^*$  leads to the same ensemble of most probable paths. Figure 8 shows the cluster's potential energy profile along two such paths. The action (and thus probability) for these two paths are the same to within one part in  $10^5$ . A third most probable path corresponds to the reflection of the pictured asymmetric path. Significantly higher actions are found for other paths obtained by quenching from dynamical configurations of the isomorphic polymer system. An example is an exchange between a central and outer particle that involves the rotation of only three disks. (The pictured paths involve rotations of four disks.)

This exploration of quenched paths reveals a mechanism for exchange involving intermediate metastable states. Indeed, when  $\langle h_A h_B(t) \rangle / \langle h_A \rangle$  is computed at a low temperature, say  $T = 0.05\varepsilon/k_B$ , no linear plateau regime is found when  $A$  and  $B$  refer to the initial and final stable states pictured in Fig.8. At these conditions, however, a linear plateau region is found when  $A$  refers to a stable state, but  $B$  refers to a metastable state. The mechanism of exchange in the cold cluster involves more than one step. Each step has a well defined rate constant.

Potential energy profiles of quenched or annealed paths for disordered many particle systems are quite different from those pictured in Fig.8. Specifically, disordered many

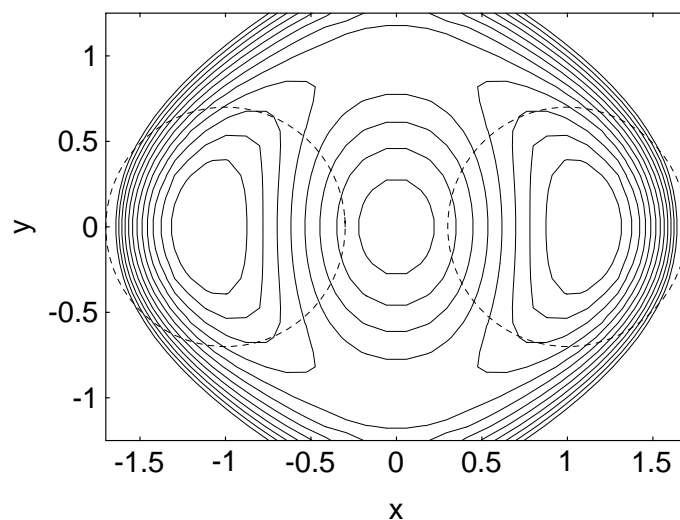


Fig. 6. – Topography of a symmetric two dimensional bi stable potential. The transition states lie  $8 k_B T$  above the stable minima. The stable states coincide with the regions contained within the dashed circles. These stable states account for 99% of the total equilibrium population.

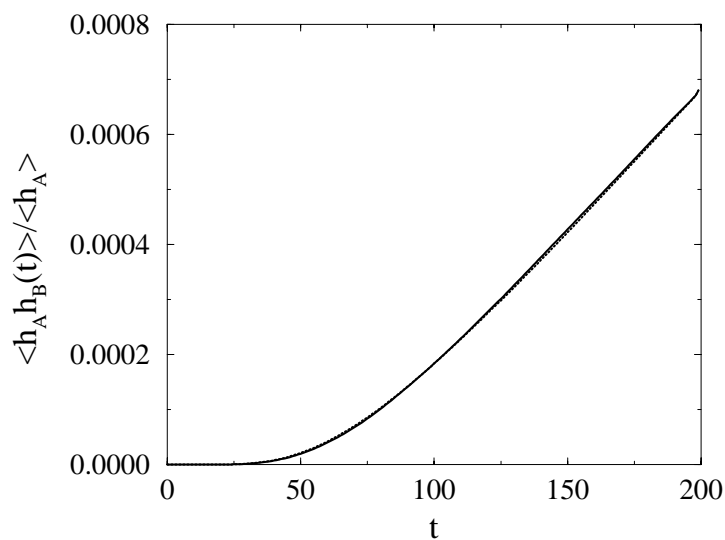


Fig. 7. – Population correlation function for dynamics in the bistable potential pictured in Fig.6. The friction constant for the dynamics is  $\gamma = 3.0$ , in reduced units. Time is in units of  $\Delta\tau$ , i.e.,  $t = \tau/\Delta\tau$ . This figure is adapted from C. Dellago, P.G.Bolhuis, F.S.Csajka and D.Chandler, *J. Chem. Phys.* **108**, 1964 (1998)

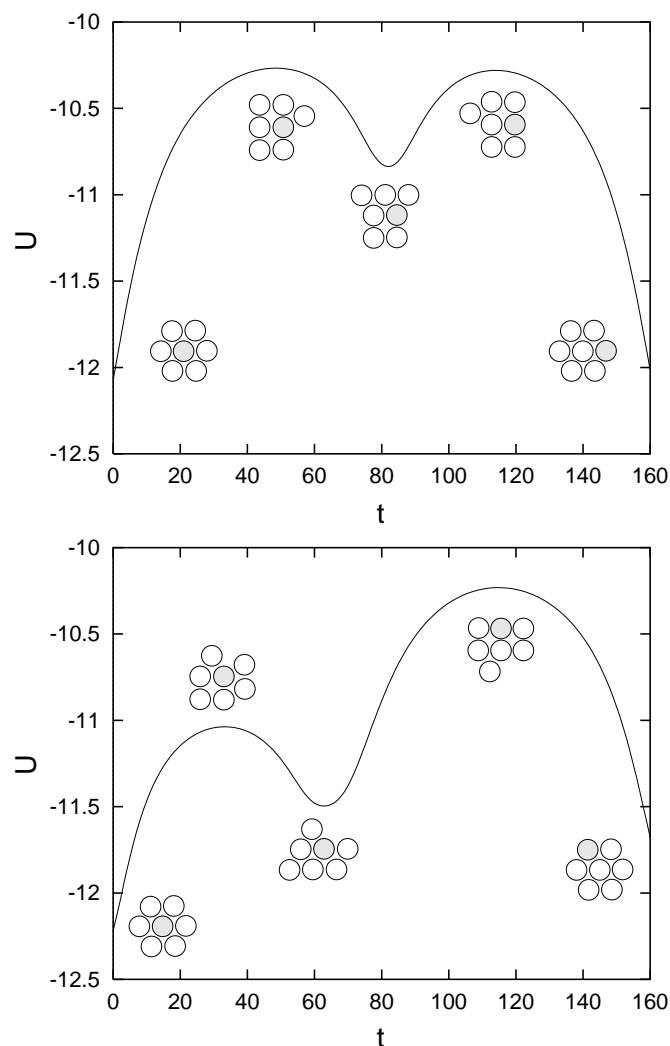


Fig. 8. – Potential energy profiles for two of the most probable paths leading to particle exchange in 160 time steps for a cold cluster of seven Lennard-Jones disks. The associated particle configurations at the points of potential energy extrema are also shown. This figure adapted from Christoph Dellago and Peter G. Bolhuis and David Chandler, *J. Chem. Phys.* **108**, 9236 (1998).

particle systems will have many local potential energy minima. Quenched paths yield a broad ensemble of rough potential energy profiles. Annealing in some of these cases can lead to narrow distributions of smooth profiles; in others, the ensemble remains broad with rough profiles. In the former case, the analysis reveals a small number of mechanisms that dominate the transition dynamics. In the latter case, the analysis reveals a frustrated transition dynamics, with a broad ensemble of possible pathways.

## 5. – Summary

Drawing chains from one stable state to another is a general realization of importance sampling for dynamics. Its advantage is obvious in that it focuses entirely upon dynamical processes of interest. With this focus, one may explore transition pathways and compute rate constants without prior knowledge of transition mechanisms.

There are, of course, challenges for future research. One serious challenge involves the issue of scale. In particular, to adopt this approach, one must pay the computational cost of treating a very large system. To study transition paths for a system with, say,  $N$  degrees of freedom, one must carry out a simulation of the isomorphic system with  $L \times N$  degrees of freedom. The chain length,  $L$ , can be of the order of  $10^2$  or  $10^3$ . (For example, in chemical dynamics applications, a typical dynamics integration time step is 1 fs, and a typical plateau time is between 0.1 and 1 ps). Thus, studying rare dynamical processes of a 100 particle system requires a simulation of a 100,000 particle system. Calculations of that scale with current computational technology can be challenging. Some relief, roughly one order of magnitude, can be found in existing algorithms that allow for large time steps in molecular dynamics. Algorithms developed to sample efficiently imaginary time quantum paths may be similarly useful.

Equilibration is another issue of significance. Imagine a process that involves several distinct classes of pathways between stable states. The energy landscape in this case will have several mountain passes, each separated from the others by substantial energy or free energy barriers. No quick straightforward dynamics will transform a chain that crosses one such pass into a chain that crosses another. In the isomorphic system, therefore, transitions between largely distinct directed polymer conformations will themselves be rare events. In such a situation, it could be difficult to obtain meaningful sampling of all transition pathways. The phenomenon is analogous to what occurs in disordered systems in states of replica broken symmetry. Systematic procedures borrowed from that area of physics may be of use here in carrying out computational analysis of transition path sampling.

\* \* \*

This lecture is based upon research carried out in collaboration with Peter Bolhuis, Felix Csajka, Christoph Dellago, Ka Lum and Jordi Marti. These people along with Gavin Crooks, Phillip Geissler, Zoran Kurtovich and Xueyu Song have provided many helpful suggestion for this lecture write-up. In addition, Gavin Crooks and Phillip Geissler provided extensive and invaluable help in preparing the manuscript. The research described in this lecture has been supported by the National Science Foundation, and by the US Department of Energy through the Chemical Sciences Division of Lawrence Berkeley Laboratory and the National Energy Research Super Computer facility.

## REFERENCES

The chain of states conception of transition pathways is similar in spirit to discretized path representation of Feynman's path integral formulation of quantum mechanics. See, for example, D. Chandler, in *Les Houches, Session LI, 1989, Liquids, Freezing and Glass Transition* ed. J.-P. Hansen, D. Levesque and J. Zinn-Justin (Elsevier Science, Amsterdam, 1991), p. 193. Some of the most powerful algorithms for sampling imaginary time quantum paths have been developed by David Ceperley, and he has described these methods in his review: D. M. Ceperley, *Rev. Mod. Phys.* **67**, 279 (1995).

Imaginary time path integral formulation of quantum theory is isomorphic to the path integral formulation of diffusion. See, for example, Chapter 2 in F. W. Wiegel, *Introduction to Path-Integral Methods in Physics and Polymer Science* (World Scientific, Singapore, 1986).

The dissociation of NaCl in water is an example where studying chains of states could be useful. In particular, when the Na-Cl separation is chosen as the reaction coordinate, the resulting transmission coefficient is very small, thus indicating the importance of other coordinates. Estimates of the small transmission coefficient computed in this way, i.e., from Eq.(1) with  $r$  given by the Na-Cl separation, were reported by O. A. Karim and J. A. McCammon, *Chem. Phys. Lett.* **132**, 219 (1986). A more detailed calculation illustrating some of the solvent's role in the dissociation pathway is given by R. Ray and E. Guàrdia, *J. Phys. Chem.* **96**, 4712 (1992).

Lawrence Pratt's seminal suggestions for studying chains of states are found in L. R. Pratt, *J. Chem. Phys.* **85**, 5045(1986). There are several applications of these and related ideas. Examples include R. Elber and M. Karplus, *Chem. Phys. Lett.* 139, 375 (1987); R. Czerminski and R. Elber, *J. Chem. Phys.* **92**, 5580 (1990); R. E. Gillilan and K. R. Wilson, *J. Chem. Phys.* **97**, 1757 (1992); E. M. Sevick, A. T. Bell and D. N. Theodorou, *J. Chem. Phys.* **98**, 3196 (1993); G. Mills and H. Jónsson, *Phys. Rev. Lett.* **72**, 1124 (1994).

The focus in these works, including Pratt's, is the discovery of specific pathways or reaction coordinates, rather than the generation of an ensemble of trajectories from which time correlation functions and rates can be computed. As such, little if any attention is paid to whether the path functionals are consistent with a specific dynamics and Liouville's theorem. Pratt, for example, suggested using a Monte Carlo action that omits the  $Q$ -factor term of Eq.(14). With that omission, the generated paths do not obey detailed balance. The first application consistent with dynamic reversibility seems to be a study of critical dynamics of an Ising model, M. Zimmer, *Phys. Rev. Lett.* **75**, 1431 (1995). Transition path sampling of *deterministic* Newtonian trajectories was first introduced and demonstrated by P. G. Bolhuis, C. Dellago and D. Chandler, *Faraday Discuss.* **110**, 421 (1998).